Article

Cell
PRESS

Discovery of Potent and Reversible Monoacylglycerol Lipase Inhibitors

Alvin R. King,[1,5] Emmanuel Y. Dotsey,[1,5] Alessio Lodola,[2] Kwang Mook Jung,[1] Azar Ghomian,[1] Yan Qiu,[3] Jin Fu,[1] Marco Mor,[2] and Daniele Piomelli[1,4,*]
[1]Department of Pharmacology, University of California Irvine, Irvine, CA 92697, USA
[2]Pharmaceutical Department, University of Parma, Parma 43100, Italy
[3]Department of Pharmacology, Xiamen University, Xiamen 361005, China
[4]Drug Discovery and Development, Italian Institute of Technology, Genova 16163, Italy
[5]These authors contributed equally to this work
*Correspondence: piomelli@uci.edu

SUMMARY

Monoacylglycerol lipase (MGL) is a serine hydrolase involved in the biological deactivation of the endocannabinoid 2-arachidonoyl-*sn*-glycerol (2-AG). Previous efforts to design MGL inhibitors have focused on chemical scaffolds that irreversibly block the activity of this enzyme. Here, we describe two naturally occurring terpenoids, pristimerin and euphol, which inhibit MGL activity with high potency (median effective concentration, IC_{50} = 93 nM and 315 nM, respectively) through a reversible mechanism. Mutational and modeling studies suggest that the two agents occupy a common hydrophobic pocket located within the putative lid domain of MGL, and each reversibly interacts with one of two adjacent cysteine residues (Cys^{201} and Cys^{208}) flanking such pocket. This previously unrecognized regulatory region might offer a molecular target for potent and reversible inhibitors of MGL.

INTRODUCTION

2-Arachidonoyl-*sn*-glycerol (2-AG), an endogenous lipid agonist for cannabinoid (CB) receptors (Sugiura et al., 1995; Mechoulam et al., 1995; Stella et al., 1997), is thought to modulate excitatory neurotransmission in the central nervous system by acting as a synaptic messenger (Katona and Freund, 2008). Electrophysiological, pharmacological, and neuroanatomical evidence suggests that 2-AG is produced in dendritic spines of glutamatergic synapses and crosses the synaptic cleft in a retrograde direction to activate presynaptic CB_1 receptors and inhibit glutamate release (Katona and Freund, 2008). CB_1-bearing axon terminals also contain the enzyme monoacylglycerol lipase (MGL) (Gulyas et al., 2004), a cytosolic serine hydrolase (Karlsson et al., 1997) that cleaves 2-AG and presumably terminates its transsynaptic actions (Dinh et al., 2002).

MGL belongs to the ''α/β hydrolase fold'' family of enzymes, whose conserved three-dimensional structures consist of a central β sheet surrounded by a variable number of α helices (Ollis et al., 1992). The active sites of these proteins are located in turns between α helices and β sheets and harbor a classic catalytic triad composed of a serine, a carboxylic acid, and a histidine (Ollis et al., 1992). Structure-alignment and site-directed mutagenesis studies have identified residues Ser^{122}, Asp^{239}, and His^{269} as the catalytic triad in rodent MGL (Karlsson et al., 1997) Moreover, mass spectrometry experiments have shown that the substituted tetrazole AM6701 (5-[(biphenyl-4-yl)methyl]-*N,N*-dimethyl-2*H*-tetrazole-2-carboxamide) inhibits human MGL by covalently modifying the enzyme's catalytic serine (Zvonok et al., 2008).

In addition to the Ser-Asp-His triad, 3 cysteine residues appear to contribute in important ways to the regulation of MGL function. Computational models position one of these residues, Cys^{242}, in close proximity of the catalytic triad, whereas mutational analyses indicate that its replacement with glycine causes a substantial loss of catalytic activity (King et al., 2009). Two additional regulatory cysteines, Cys^{201} and Cys^{208}, are found on the putative lid domain of MGL, a flexible structure that is thought to function as an entry gate to the active site of this and other lipases (Jaeger et al., 1999). Though mutations affecting Cys^{201} and Cys^{208} produce only a moderate decrease in MGL activity, they markedly reduce the ability of cysteine-reacting agents to inhibit such activity (King et al., 2009).

The presence of MGL in glutamatergic axon terminals (Gulyas et al., 2004) suggests that this enzyme might be involved in the termination of 2-AG-mediated retrograde transmission at excitatory synapses. This idea is supported by studies showing that virally induced MGL overexpression reduces receptor-dependent 2-AG accumulation in primary cultures of rat brain neurons (Dinh et al., 2002), and that siRNA-mediated MGL silencing increases 2-AG levels in HeLa cells (Dinh et al., 2004). Pharmacological experiments in vivo have provided further support for a role of MGL in 2-AG deactivation. Microinjections of the carbamate-based MGL inhibitor URB602 (biphenyl-3-ylcarbamic acid cyclohexyl ester) into the periaqueductal gray region of the midbrain increased 2-AG levels and enhanced stress-induced analgesia in rats (Hohmann et al., 2005). Moreover, local or systemic URB602 administration reduced nocifensive responses elicited in rodents by experimental nerve injury (Desroches et al., 2008) and by injections of formalin (Guindon et al., 2007) or carrageenan (Comelli et al., 2007). More recently, the potent carbamate-based MGL inhibitor JZL-184 (4-(bis-benzo[1,3]dioxol-5-yl-hydroxy-methyl)-piperidine-1-carboxylic acid 4-nitro-phenyl ester) was shown to produce a classical set

of cannabinoid-like responses—including decreases in pain behavior, body temperature, and motor activity—when injected in mice (Long et al., 2009a). Administration of JZL-184 also elevates 2-AG levels in peripheral tissues, highlighting the important role of MGL in the hydrolysis of 2-AG outside the brain (Long et al., 2009b), where this endocannabinoid was originally discovered (Mechoulam et al., 1995).

All potent inhibitors of MGL activity reported thus far—including carbamates (Long et al., 2009a, 2009b; Muccioli et al., 2008), maleimides (Saario et al., 2005), tetrazoles (Zvonok et al., 2008), and isothiazolinones (King et al., 2009)—exert their effects by forming covalent bonds with reactive serine or cysteine residues. Because there are potential clinical disadvantages to this mode of action, in the present study we screened a commercial chemical library to identify scaffolds that might be utilized to design reversible MGL inhibitors. We describe the discovery of two bioisosteric terpenoids, pristimerin and euphol, which inhibit MGL with high potency by interacting in a reversible manner with a novel regulatory region of MGL.

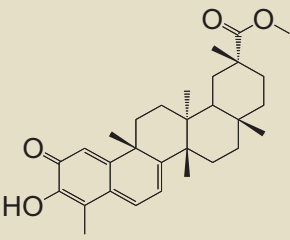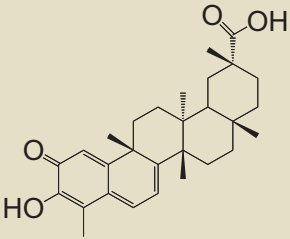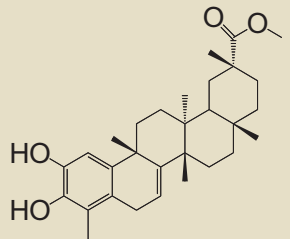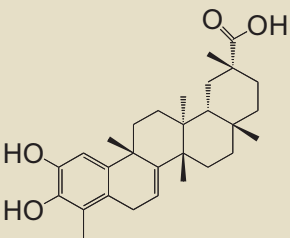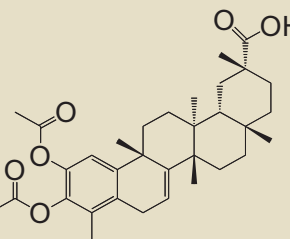## RESULTS AND DISCUSSION

Pristimerin Inhibits MGL

The screening of the chemical library revealed the presence of multiple active compounds. Because of its high potency, we selected for further studies the friedelane triterpenoid, pristimerin (Table 1) (Dev et al., 1989). Pristimerin inhibited the activity of purified MGL with a median effective concentration (IC_{50}) of 93 ± 8 nM (mean and standard error of the mean [SEM]; n = 3) and that of nonpurified MGL (cell lysates of MGL-transfected HeLa cells) with an IC_{50} of 398 ± 68 nM (n = 4) (Figure 1A). The difference in potency observed between these two preparations might reflect the presence of competing reactions in the crude HeLa extract and/or inadequate posttranslational modifications of the *E. coli* protein.

Other friedelane triterpenoids represented in the library also inhibited MGL activity, albeit less potently than pristimerin did. These included celastrol, pristimerol, dihydrocelastrol, and dihydrocelastryl diacetate (Table 1). The inhibitory potencies of these compounds appeared to be particularly sensitive to chemical modifications at the two opposite ends of their rigid terpenoid scaffold: the esterification of the carboxyl group at carbon 29, which increased inhibitory activity, and the reduction of the quinone methide ring, which decreased such activity (Table 1).

### Pristimerin Is a Reversible MGL Inhibitor

The quinone methide group tends to react with cysteine residues in proteins to form covalent adducts (Bolton et al., 1997). To determine whether pristimerin might act through a similar mechanism, we studied the interaction of this compound with purified MGL using a rapid dilution assay (King et al., 2009; Copeland, 2005). Under the conditions of this test, incubation of MGL with a covalent inhibitor—for example, the serine-reactive agent methyl arachidonylfluorophosphonate (MAFP)—resulted in the formation of an enzyme-inhibitor complex that is resistant to dilution of the assay mixture (Figure 1B) (King et al., 2009). By contrast, rapid dilution of the MGL-pristimerin mixture resulted in a virtually complete recovery of catalytic activity, which is

Table 1. Inhibition of Purified Recombinant MGL by Friedelane-Based Pentacyclic Triterpenoids

Compound	Structure	IC_{50}
1 Pristimerin		93 ± 8 nM
2 Celastrol		1.6 ± 0.4 μM
3 Pristimerol		4 ± 0.5 μM
4 Dihydrocelastrol		15 ± 4 μM
5 Dihydrocelastryl Diacetate		15 ± 3 μM

Results are expressed as mean ± SEM (n = 3–4).

suggestive of a reversible inhibition (Figure 1B). Time-course experiments showed that addition of pristimerin to purified MGL produces an almost immediate blockade of MGL activity (Figure 1C). Additional kinetic studies using nonpurified HeLa MGL demonstrated that pristimerin decreases the maximal
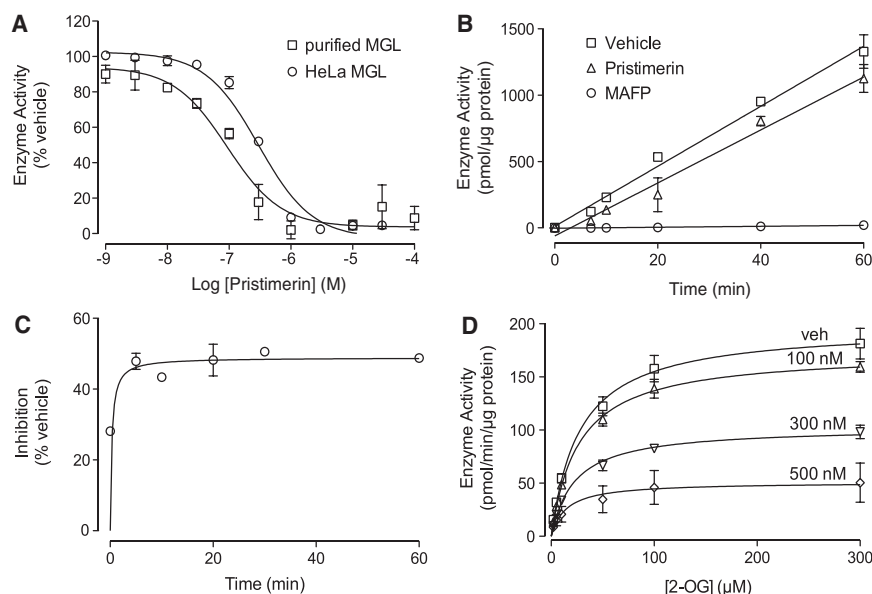
Figure 1. Pristimerin Inhibits MGL

(A) Concentration-dependent inhibition of purified MGL (squares, n = 3) and HeLa MGL (circles, n = 4) by pristimerin.

(B) Rapid dilution assays of HeLa-MGL in the presence of vehicle (squares, DMSO, final concentration 2%), pristimerin (triangles), or MAFP (circles). We measured the amount of reaction product (pmol/μg protein) generated over a 60 min period following a 20 min preincubation with inhibitor or vehicle (n = 3).

(C) Time course of MGL inhibition by pristimerin (300 nM, n = 3).

(D) Michaelis-Menten analysis of the MGL reaction (measured as pmol/min/μg protein) in the presence of vehicle (squares, DMSO, 1%) (n = 4) or pristimerin (100 nM, 300 nM, or 500 nM; n = 3–4). Enzyme activity is reported as percent of vehicle controls (DMSO, 1%). Results are expressed as mean ± SEM, with each assay performed in duplicate.

catalytic velocity of this enzyme (V_{max} in pmol/min/μg; vehicle, 200 ± 20, n = 11; 100 nM, 174 ± 7, n = 3; 300 nM, 104 ± 7, n = 4; 500 nM, 51 ± 18, n = 3; $p < 0.005$) without influencing its Michaelis-Menten constant (K_m in μM; vehicle, 28 ± 4; 100 nM, 27 ± 1; 300 nM, 24 ± 5; 500 nM, 14 ± 2; $p > 0.3$) (Figure 1D). Together, the results indicate that pristimerin inhibits MGL through a mechanism that is rapid, reversible, and noncompetitive.
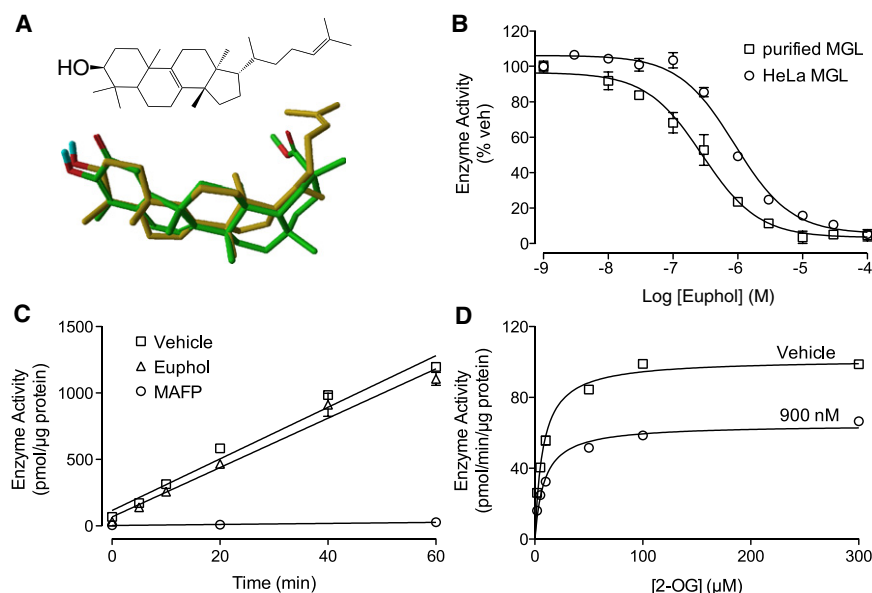
Euphol Is a Bioisoster of Pristimerin

To further evaluate the role of the quinone methide group, we examined whether bioisosters of pristimerin that lack this moiety might also inhibit MGL activity. A computational analysis of structures represented in the chemical library revealed that the triterpene alcohol, euphol (Dev et al., 1989), takes a minimum

energy conformation that is superimposable to the rigid scaffold of pristimerin, allowing the hydroxyl groups of the two molecules to overlap (Figure 2A). Enzyme assays showed that euphol inhibits purified MGL with an IC_{50} of 315 ± 1 nM (n = 3) and non-purified HeLa MGL with an IC_{50} of 882 ± 78 nM (n = 3) (Figure 2B). Moreover, rapid dilution and kinetic experiments demonstrated that euphol blocks MGL activity through a reversible and non-competitive mechanism, which is apparently identical to that of pristimerin (Figures 2C and 2D).

Interactions with Regulatory Cysteines: Modeling Studies

The structural and mechanistic similarities between pristimerin and euphol prompted us to examine whether the two

Figure 2. Euphol Is a Bioisoster of MGL

(A) Chemical structure of euphol (top) and three-dimensional superposition of euphol (gold) and pristimerin (green). Oxygens, red; hydrogens, blue.

(B) Concentration-dependent inhibition of purified MGL (squares) and HeLa MGL (circles) by euphol. Enzyme activity is reported as percent of vehicle controls (DMSO, 1%). Results are expressed as mean ± SEM (n = 3).

(C) Rapid dilution assays of HeLa-MGL in the presence of vehicle (squares, DMSO, final concentration 2%), euphol (triangles), or MAFP (circles). We measured the amount of reaction product (pmol/μg protein) generated over a 60 min period following a 20 min preincubation with inhibitor or vehicle. Results are expressed as mean ± SEM (n = 3).

(D) Michaelis-Menten analysis of the MGL reaction in the presence of vehicle (squares, DMSO, 1%) (n = 4) or euphol (900 nM). Results are expressed as mean ± SEM (n = 3).
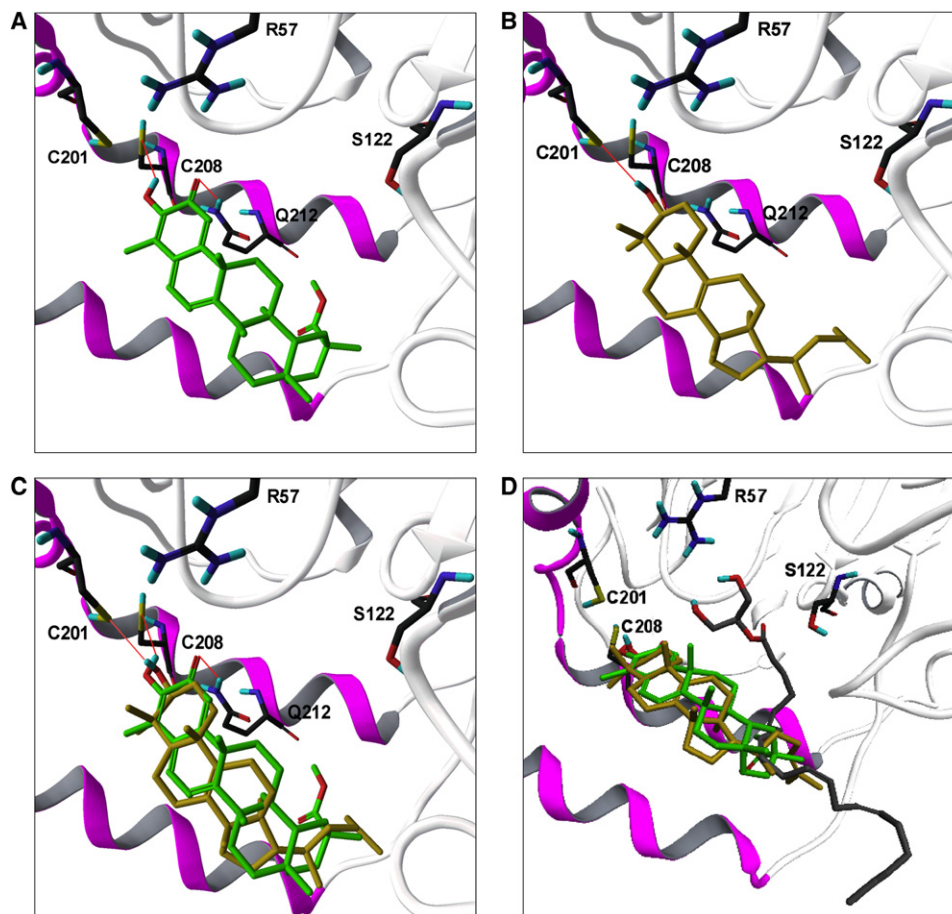
Figure 3. Interaction of Pristimerin and Euphol with Regulatory Cysteines

(A and B) Predicted binding modes of pristimerin (A) and euphol (B) to the model of rat MGL, showing their possible interactions with Cys[208] and Cys[201]. The docking pose adopted by pristimerin predicts an additional interaction with a neighboring glutamine residue (Gln[212]).

(C) Superposition of the two models.

(D) Docking pose for 2-AG in the presumptive active site of MGL [10] along with the putative region of overlap with pristimerin and euphol. MGL carbons black; pristimerin, green; euphol, gold; 2-AG, gray; oxygens, red; hydrogens, blue; sulfurs, yellow; nitrogens, dark blue; lid domain, magenta; α/β core, white.

compounds might interact with a common binding pocket in MGL. As a first test of this hypothesis, we utilized an induced-fit docking (IFD) protocol (Sherman et al., 2006) to compare the binding poses adopted by pristimerin and euphol in a refined computational model of MGL (King et al., 2009; Saario et al., 2005). Figure 3A illustrates a docking solution for pristimerin in which the lipophilic portion of the molecule lies on a pocket located within the lid domain of MGL and its 3-hydroxyl group faces the regulatory cysteines, Cys[201] and Cys[208] (King et al., 2009). This solution was further probed using molecular dynamics (MD) simulations. Starting from the orientation depicted in Figure 3A, pristimerin was found to oscillate around its initial conformation with a ligand atom root-mean-square distance (RMSD) of 0.36 ± 0.08 Å. Average distances between the polar hydrogen of the 3-hydroxyl group of pristimerin and the sulfur atoms of Cys[208] and Cys[201] were 2.90 ± 0.25 Å and 3.22 ± 0.27 Å, respectively. This suggests that the binding of pristimerin to MGL might be strengthened by formation of a polar interaction with a regulatory cysteine, possibly Cys[208].

A subsequent set of IFD analyses showed that euphol can be readily superposed on pristimerin so that its 3-hydroxyl group faces Cys[208] and Cys[201] (Figure 3B,C). Notably, however, the interaction of euphol with Cys[208] was lost in the early phase of the simulation (average hydrogen-sulfur distance = 4.00 ± 0.31 Å), whereas the interaction with Cys[201] turned out to be significantly more stable (average hydrogen-sulfur distance, 3.13 ± 0.39 Å). During MD simulations, euphol had a higher RMSD compared with pristimerin (0.96 ± 0.09 Å), mainly owing to a change in the conformation of its tail at C17. A plausible interpretation of these results is that pristimerin and euphol occupy a common hydrophobic pocket within the lid domain of MGL, and each inhibitor engages through polar interactions 1 of 2 adjacent cysteine residues, Cys[201] and Cys[208], which flank this pocket. The limited overlap of the region occupied by pristimerin and euphol with the presumptive active site of MGL (Figure 3D) is consistent with the noncompetitive kinetic behavior displayed by these inhibitors. However, there are other possible explanations for such behavior, including
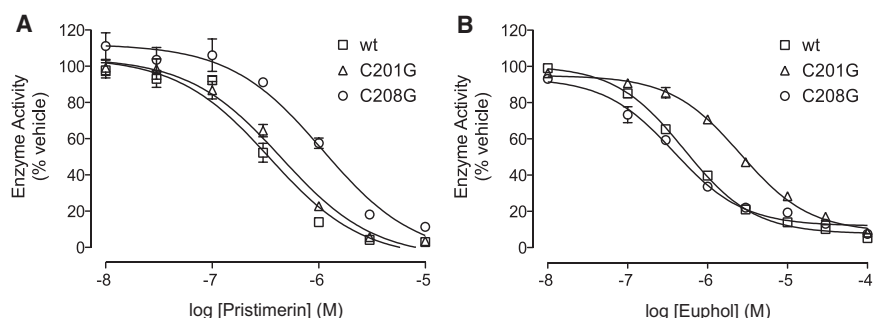
Figure 4. Effect of Cysteine Mutations on MGL Inhibition by Pristimerin and Euphol

Effects of mutating Cys^{201} or Cys^{208} on MGL inhibition by pristimerin (A) and euphol (B). Concentration-response curves for the inhibition of wild-type MGL (wt, squares) and MGL mutants containing cysteine-to-glycine mutations at either Cys^{201} (C201G, triangles) or Cys^{208} (C208G, circles). Enzyme activity is reported as percent of vehicle controls (DMSO, 1%). Results are expressed as mean ± SEM (n = 4-9). $p < 0.0001$, ANOVA, followed by Dunnett's test.

stabilization of a conformation of MGL that is inaccessible to the substrate.

Interaction with Regulatory Cysteines: Mutational Analyses

A prediction of our theoretical model is that mutations affecting either Cys^{208} or Cys^{201} should differentially affect the inhibitory potencies of pristimerin and euphol. To test this possibility, we mutated the two cysteines into glycines, expressed the mutants in HeLa cells, and determined the inhibitory effects of pristimerin and euphol on MGL activity in cell extracts. The replacement of Cys^{208} caused a marked rightward shift in the concentration-response curve for pristimerin (Figure 4A) (IC_{50}; wt = 350 ± 37 nM; C208G = 1182 ± 174 nM; n = 6; $p < 0.0001$), whereas it had no effect on euphol (Figure 4B). Conversely, a mutation affecting Cys^{201} significantly reduced the inhibitory potency of euphol (Figure 4B) (IC_{50}; wt = 513 ± 9 nM; C201G = 2601 ± 200 nM; n = 4; $p < 0.0001$) without affecting the potency of pristimerin (Figure 4A). Mutating a cysteine residue that is distant from both active site and lid domain, Cys^{32}, did not influence the activity of either agent (data not shown). The results support the validity of the computational model illustrated in Figure 3D, suggesting that reversible interactions of pristimerin and euphol with Cys^{208} and Cys^{201}, respectively, contribute to the inhibitory potencies of these two agents.

Effects of Pristimerin in Intact Rat Brain Neurons

We next asked whether reversible inhibition of MGL activity, such as that produced by pristimerin and euphol, might effectively protect 2-AG from degradation in intact brain neurons, which contain relatively high concentrations of 2-AG and other monoacylglycerols that are substrates for MGL. Incubation of primary cultures of rat cortical neurons with the cysteine-reactive MGL inhibitor, N-arachidonylmaleimide (1 μM, 25 min) (Saario et al., 2005), increased the levels of 2-AG and palmitoylethanolamide (PEA), a noncannabinoid fatty-acid ethanolamide that is primarily hydrolyzed, in neurons, by fatty-acid amide hydrolase (FAAH) (Figure 5) (Désarnaud et al., 1995; Cravatt et al., 1996). Under the same experimental conditions, incubation with pristimerin (1 μM, 30 min) caused an elevation in cellular 2-AG concentrations (1.6 ± 0.1 fold change, n = 3), which was not accompanied by any significant changes in PEA (Figure 5). As expected from its weaker inhibitory potency, euphol (10 μM, 30 min) caused a small, nonsignificant change in the levels of 2-AG (1.2 ± 0.2 fold change, n = 3) and PEA (data not shown).

The results described above suggest that pristimerin preferentially inhibits 2-AG hydrolysis in intact brain neurons. Consistent with this conclusion, a survey of endocannabinoid-metabolizing enzymes showed that pristimerin had no significant effect, in vitro, on the activities of rat brain diacylglycerol lipase (a serine hydrolase responsible for the production of 2-AG) (Bisogno et al., 2003), rat brain FAAH, and rat recombinant N-acylethanolamide acid amidase (a cysteine amidase involved in the degradation of PEA and other fatty-acid ethanolamides) (see Table S1 available online) (Cravatt et al., 1996; Ueda et al., 2001). Though pristimerin did not affect the activity of the 2-AG hydrolase ABHD12, it was potent at inhibiting the activity of another 2-AG-hydrolyzing enzyme, ABHD6 (IC_{50} = 98 ± 8 nM, n = 3) (Blankman et al., 2007). ABHD6 displays a closer sequence homology with MGL than ABHD12 does (in sequence similarity; MGL and ABHD6, 33%; ABHD6 and ABHD12, 26.3%). Euphol produced a similar, albeit weaker inhibitory effect on ABHD6 (IC_{50} = 9 ± 1 μM, n = 6).

SIGNIFICANCE

MGL is localized to axon terminals throughout the brain and is thought to participate in the physiological elimination of
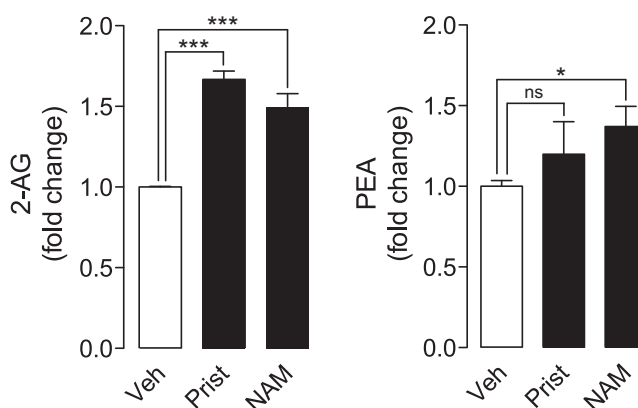

Figure 5. Pristimerin Protects 2-AG from Degradation in Neurons

Effects of pristimerin (1 μM), NAM (1 μM), or vehicle (0.1% DMSO in DMEM) in primary cultures of rat cortical neurons. Levels of 2-AG and PEA are reported as fold change over vehicle-treated neurons. Results are expressed as mean ± SEM (n = 5). ****$p < 0.0001$, ***$p < 0.001$, *$p < 0.05$, ns = not significant, unpaired Student's t test.

2-AG at central synapses. Consistent with this view, pharmacological blockade of MGL activity exerts multiple effects in live animals, including profound antinociception in models of acute and chronic pain. The irreversible mechanism of action of all potent MGL inhibitors described so far presents, however, possible clinical issues (e.g., the formation of antigenic adducts with plasma proteins) that might eventually hinder the therapeutic use of these agents. To overcome these potential limitations, in the present study we screened a commercial chemical library to identify structural motifs that might be utilized as a starting point for the design of reversible MGL inhibitors. Our screen led to the discovery of two bioisosteric terpenes, pristimerin and euphol, which inhibit MGL activity through a reversible mechanism and with high potency in vitro. Investigations into the inhibitory properties of these agents—utilizing a combination of biochemical, molecular modeling, and mutagenesis approaches—suggest that they occupy a common hydrophobic pocket located within the α-helical lid domain of MGL, and each interacts reversibly with either of 2 neighboring cysteines present at the border of such pocket: Cys[201] and Cys[208]. Notably, prior studies had already implicated these residues in the covalent inhibition of MGL by isothiazolinone derivatives (King et al., 2009). The identification of this regulatory region of MGL provides a novel molecular target for the generation of potent and reversible inhibitors.

EXPERIMENTAL PROCEDURES

Chemicals

Compounds **1-6** were part of the Spectrum Collection, purchased from MicroSource Discovery Systems Inc. (Gaylordsville, CT). MAFP and NAM were obtained from Cayman Chemical (Ann Arbor, MI), 2-oleoyl-*sn*-glycerol (2-OG) from Indofine Chemical (Hillsborough, NJ), and 2-[^{2}H$_8$]-AG from Cayman Chemical; [^{2}H$_4$]-PEA was synthesized as described previously (Fegley et al., 2005).

Screening for MGL Inhibitors

The Spectrum Collection (MicroSource Discovery Systems, retrieved May 20, 2009, from http://www.msdiscovery.com/home.html) is composed of 2000 compounds, supplied in a 10 mM dimethyl sulfoxide (DMSO) solution. We pooled groups of 10 compounds and performed a primary screen at a concentration of 1 μM. Individual compounds from positive groups (≥50% MGL inhibition) were subjected to a secondary screen at 10 μM. Full concentration-inhibition curves were generated using new lots of dry compounds.

Enzyme Assays

Purified recombinant rat MGL was prepared and enzyme activity was assayed as described previously (King et al., 2007). Full-length rat ABHD6 or ABHD12 was subcloned into a pEF-V5/His vector by TOPO cloning (Invitrogen, Carlsbad, CA) and verified by DNA sequencing. HeLa cells were transiently transfected with pEF6 vector, ABHD6-V5-pEF6 or ABHD12-V5-pEF6 using Superfect reagent (QIAGEN, Valencia, CA). Forty-eight hours after transfection, cells were harvested and the homogenates were prepared in 50 mM Tris-Cl (pH 8.0) containing 0.32 M sucrose. ABHD activity was measured using a modified MGL assay procedure (pH 7.5, 3 μg protein per reaction, 30 min at 37°C) (King et al., 2007). Samples were extracted (King et al., 2007) and analyzed by liquid chromatography/mass spectrometry (LC/MS) (see below). 2-AG-hydrolase activity (in pmol/min/mg protein) in mock-transfected HeLa cells was 1.4 ± 0.05, in pEF6-transfected (vector only) was 1.3 ± 0.01, and in ABHD6-transfected cells was 6.9 ± 0.2 (n = 3). FAAH and DGL activities were measured in rat brain homogenates as described elsewhere (Stella et al., 1997). Recombinant NAAA protein was prepared from HEK293 cells stably transfected with pCMV-Flag-rNAAA using SuperFect reagent (QIAGEN)

and screened with G418 (0.3 mg/ml). Cells were harvested and sonicated in 20 mM Tris-HCl (pH 7.5) with 0.32 M sucrose, centrifuged at 800 × g for 15 min at 4°C, and supernatant was centrifuged at 12,000 × g for 30 min at 4°C. The pellet was suspended in phosphate-buffered saline (PBS) and subjected to 2 freeze-thaw cycles at −80°C. The suspension was centrifuged at 105,000 × g for 1 hr at 4°C, and the supernatant containing rNAAA was kept at −80°C until use. NAAA activity was measured by combining substrate (50 μM heptadecenoylethanolamide) with protein (10 μg) in assay buffer (50 mM sodium hydrogen phosphate buffer [pH 5.0], 0.1% Triton X-100, 3 mM DTT) in a final volume of 0.2 ml for 30 min at 37°C. Reactions were stopped by addition of 0.2 ml cold methanol containing 1 nmol heptadecanoic acid (NuChek Prep, Elysian, MN). For MGL, ABHD, and NAAA assays, samples were analyzed by LC/MS on an XDB Eclipse C18 column (2.1 × 30 mm i.d., 1.8 μm,) at 0.6 ml/min for 0.6 min with a solvent mixture of 95% methanol and 5% water, both containing 0.25% acetic acid and 5 mM ammonium acetate. The column temperature was 50°C. Samples were analyzed by electrospray ionization in the negative mode. Capillary voltage was 4 kV, fragmentor voltage was 100 V, nebulizer pressure was 60 psi. N$_2$ was used as drying gas at a flow rate of 13 l/min and a temperature of 350°C. We monitored the appropriate enzyme activity product (MGL and ABHD, m/z = 281, NAAA, m/z = 267) in the selected ion monitoring mode using heptadecanoic acid as standard (m/z = 269).

Site-Directed Mutagenesis

Generation of cysteine-to-glycine point mutants by site-directed mutagenesis and subsequent transfections in HeLa cells were performed as previously described (King et al., 2009).

Neuron Cultures

Primary cortical neuron cultures were prepared from embryonic day 18-20 Wistar rats (Stella and Piomelli, 2001). Cultures were maintained for 10 days at 37°C with 5% CO$_2$ before treatment with pristimerin (1 μM), euphol (10 μM), NAM (1 μM), or vehicle (0.1% DMSO in Dulbecco's modified Eagle medium [DMEM]) for 30 min at 37°C. Reactions were stopped by washing with ice-cold PBS and cells were harvested in 2 ml 50% methanol. Lysates were vortexed for 10 s, protein concentrations were measured by bicinchoninic acid protein assay (Pierce, Rockford, IL), and samples were extracted in 4 ml ice-cold methanol/chloroform/water (1:2:1, vol:vol:vol) containing 0.5 nmol 2-[^{2}H$_8$]-AG, and 10 pmol each of [^{2}H$_4$]-PEA, added as internal standard. Organic phases were recovered, evaporated under N$_2$, reconstituted in 50 μl chloroform/methanol (1:3, vol:vol), and analyzed by LC/MS as described previously (Astarita and Piomelli, 2009).

Computational Modeling

Docking studies were carried out using the IFD approach (King et al., 2009) based on *Prime 1.7* (Schrödinger, LLC, New York, NY) and *Glide 5.0* (Schrödinger, LLC, New York, NY) molecular modeling software. Coordinates of rat MGL were taken from a previously published model of the enzyme in complex with 2-AG (King et al., 2009). Inhibitors were built using *Maestro 8.5* (Schrödinger, LLC) and their geometries were optimized to an energy gradient of 0.01 kcal/(mol·Å) with the OPLS2005 force field (Jorgensen et al., 1996). In turns, the inhibitors were placed in an arbitrary position within a region centered on residues Cys[201], Cys[208], or Cys[242] of MGL using enclosing and bounding boxes of 20 Å and 10 Å on each side, respectively. For the IFD protocol, an initial softened-potential docking of the ligand to the rigid receptor was performed, with van der Waals radii scaling of 0.5 for both MGL and ligand nonpolar atoms. Sampling of the protein conformation for each of the top 20 ligand poses (ranked by *Glide*) was performed using *Prime*. In this phase, residues within 5 Å of the ligand pose were refined by side-chain conformational search followed by full minimization of the residues and the ligand. Complexes within 30.0 kcal/mol of minimum energy structure were taken forward for redocking. The related ligand was redocked into each low-energy, induced-fit structure with default *Glide* settings (van der Waals radii scaling of 1.0 for MGL and 0.8 for the ligand). Each complex was then ranked according to the IFD score.

Molecular dynamics simulations of the IFD complexes were performed using OPLS2005 force field in combination with the surface generalized Born (SGB) continuum model for solvent (water) representation. SHAKE

function was used and a time step of 2 fs was applied for 2 ns simulation at 300 K, after an equilibration phase of 200 ps at the same temperature. Backbone atoms were frozen during the simulations to preserve MGL tertiary structure. Interactions between the 3-hydroxyl group of the inhibitors and cysteine sulfur atoms were monitored during the simulations. Distances are reported as average values over 200 snapshots extracted from MD trajectory.

Pristimerin and euphol were aligned by a rigid fit procedure superposing the carbon atoms of ring A, B, and C. The minimum energy conformation of euphol giving the best fit in terms of RMSD was selected for modeling purpose.

SUPPLEMENTAL DATA

Supplemental data include a table and can be found with the article online at http://www.cell.com/chemistry-biology/supplemental/S1074-5521(09)00322-6.

REFERENCES

Astarita, G., and Piomelli, D. (2009). Lipidomic analysis of endocannabinoid metabolism in biological samples. J. Chromatogr. B. Analyt. Technol. Biomed. Life Sci. *877*, 2755–2767.

Bisogno, T., Howell, F., Williams, G., Minassi, A., Cascio, M.G., Ligresti, A., Matias, I., Schiano-Moriello, A., Paul, P., Williams, E.J., et al. (2003). Cloning of the first sn1-DAG lipases points to the spatial and temporal regulation of endocannabinoid signaling in the brain. J. Cell Biol. *163*, 463–468.

Blankman, J.L., Simon, G.M., and an Cravatt, B.F. (2007). A comprehensive protile of brain enzymes that hydrolyze the endocannabinoid 2-arachidonoyl-glycerol. Chem. Biol. *14*, 1347–1356.

Bolton, J.L., Turnipseed, S.B., and Thompson, J.A. (1997). Influence of quinone methide reactivity on the alkylation of thiol and amino groups in proteins: studies utilizing amino acid and peptide models. Chem. Biol. Interact. *107*, 185–200.

Comelli, F., Giagnoni, G., Bettoni, I., Colleoni, M., and Costa, B. (2007). The inhibition of monoacylglycerol lipase by URB602 showed an anti-inflammatory and anti-nociceptive effect in a murine model of acute inflammation. Br. J. Pharmacol. *152*, 787–794.

Copeland, R.A. (2005). Evaluation of Enzyme Inhibitors in Drug Discovery, R.A. Copeland, ed. (Hoboken, NJ: John Wiley and Sons, Inc.), pp. 56–63.

Cravatt, B.F., Giang, D.K., Mayfield, S.P., Boger, D.L., Lerner, R.A., and Gilula, N.B. (1996). Molecular characterization of an enzyme that degrades neuromodulatory fatty-acid amides. Nature *384*, 83–87.

Désarnaud, F., Cadas, H., and Piomelli, D. (1995). Anandamide amidohydrolase activity in rat brain microsomes. Identification and partial characterization. J. Biol. Chem. *270*, 6030–6035.

Desroches, J., Guindon, J., Lambert, C., and Beaulieu, P. (2008). Modulation of the anti-nociceptive effects of 2-arachidonoyl glycerol by peripherally administered FAAH and MGL inhibitors in a neuropathic pain model. Br. J. Pharmacol. *155*, 913–924.

Dev, S., Gupta, A.S., and Patwardhan, S.A. (1989). Handbook of Terpenoids, S. Dev, ed. (Boca Raton, FL: CRC Press, Inc.), pp. 7–62.

Dinh, T.P., Carpenter, D., Leslie, F.M., Freund, T.F., Katona, I., Sensi, S.L., Kathuria, S., and Piomelli, D. (2002). Brain monoglyceride lipase participating in endocannabinoid inactivation. Proc. Natl. Acad. Sci. USA *99*, 10819–10824.

Dinh, T.P., Kathuria, S., and Piomelli, D. (2004). RNA interference suggests a primary role for monoacylglycerol lipase in the degradation of the endocannabinoid 2-arachidonoylglycerol. Mol. Pharmacol. *66*, 1260–1264.

Fegley, D., Gaetani, S., Duranti, A., Tontini, A., Mor, M., Tarzia, G., and Piomelli, D. (2005). Characterization of the fatty acid amide hydrolase inhibitor cyclohexyl carbamic acid 3′-carbamoyl-biphenyl-3-yl ester (URB597): effects on anandamide and oleoylethanolamide deactivation. J. Pharmacol. Exp. Ther. *313*, 352–358.

Guindon, J., Desroches, J., and Beaulieu, P. (2007). The antinociceptive effects of intraplantar injections of 2-arachidonoyl glycerol are mediated by cannabinoid CB_2 receptors. Br. J. Pharmacol. *150*, 693–701.

Gulyas, A.I., Cravatt, B.F., Bracey, M.H., Dinh, T.P., Piomelli, D., Boscia, F., and Freund, T.F. (2004). Segregation of two endocannabinoid-hydrolyzing enzymes into pre- and postsynaptic compartments in the rat hippocampus, cerebellum and amygdala. Eur. J. Neurosci. *20*, 441–458.

Hohmann, A.G., Suplita, R.L., Bolton, N.M., Neely, M.H., Fegley, D., Mangieri, R., Krey, J.F., Walker, M., Holmes, P.V., Crystal, J.D., et al. (2005). An endocannabinoid mechanism for stress-induced analgesia. Nature *435*, 1108–1112.

Jaeger, K.E., Dijkstra, B.W., and Reetz, M.T. (1999). Bacterial biocatalysts: molecular biology, three-dimensional structures, and biotechnological applications of lipases. Annu. Rev. Microbiol. *53*, 315–351.

Jorgensen, W.L., Maxwell, D.S., and Tirado-Rives, J. (1996). Development and testing of the OPLS all-atom force field on conformational energetics and properties of organic liquids. J. Am. Chem. Soc. *118*, 11225–11236.

Karlsson, M., Contreras, J.A., Hellman, U., Tornqvist, H., and Holm, C. (1997). cDNA cloning, tissue distribution, and identification of the catalytic triad of monoglyceride lipase. Evolutionary relationship to esterases, lysophospholipases, and haloperoxidases. J. Biol. Chem. *272*, 27218–27223.

Katona, I., and Freund, T.F. (2008). Endocannabinoid signaling as a synaptic circuit breaker in neurological disease. Nat. Med. *14*, 923–930.

King, A.R., Duranti, A., Tontini, A., Rivara, S., Rosengarth, A., Clapper, J.R., Astarita, G., Geaga, J., Luecke, H., Mor, M., et al. (2007). URB602 inhibits monoacylglycerol lipase and selectively blocks 2-arachidonoylglycerol degradation in intact brain slices. Chem. Biol. *14*, 1357–1365.

King, A.R., Lodola, A., Carmi, C., Fu, J., Mor, M., and Piomelli, D. (2009). A critical cysteine residue in monoacylglycerol lipase is targeted by a new class of isothiazolinone-based enzyme inhibitors. Br. J. Pharmacol. *157*, 974–983.

Long, J.Z., Li, W., Booker, L., Burston, J.J., Kinsey, S.G., Schlosburg, J.E., Pavon, F.J., Serrano, A.M., Selley, D.E., Parsons, L.H., et al. (2009a). Selective blockade of 2-arachidonoylglycerol hydrolysis produces cannabinoid behavioral effects. Nat. Chem. Biol. *5*, 37–44.

Long, J.Z., Nomura, D.K., and Cravatt, B.F. (2009b). Characterization of monoacylglycerol lipase inhibition reveals differences in central and peripheral endocannabinoid metabolism. Chem. Biol. *16*, 744–753.

Mechoulam, R., Ben-Shabbat, S., Hanus, L., Ligumsky, M., Kaminski, N., Schatz, A.R., Gopher, A., Almog, S., Martin, B.R., Compton, D.R., et al. (1995). Identification of an endogenous 2-monoglyceride, present in canine gut, that binds to cannabinoid receptors. Biochem. Pharmacol. *50*, 83–90.

Muccioli, G.G., Labar, G., and Lambert, D.M. (2008). CAY10499, a novel monoglyceride lipase inhibitor evidenced by an expeditious MGL assay. ChemBioChem *9*, 2704–2710.

Ollis, D.L., Cheah, E., Cygler, M., Dijkstra, B., Frolow, F., Franken, S.M., Harel, M., Remington, S.J., Silman, I., Schrag, J., et al. (1992). The α/β hydrolase fold. Protein Eng. *5*, 197–211.

Saario, S.M., Salo, O.M.H., Nevalainen, T., Poso, A., Laitinen, J.T., Järvinen, T., and Niemi, R. (2005). Characterization of the sulfhydryl-sensitive site in the enzyme responsible for hydrolysis of 2-arachidonoyl-glycerol in rat cerebellar membranes. Chem. Biol. *12*, 649–656.

Sherman, W., Day, T., Jacobson, M.P., Friesner, R.A., and Farid, R. (2006). Novel procedure for modeling ligand/receptor induced fit effects. J. Med. Chem. *49*, 534–553.

Stella, N., and Piomelli, D. (2001). Receptor-dependent formation of endogenous cannabinoids in cortical neurons. Eur. J. Pharmacol. *425*, 189–196.

Stella, N., Schweitzer, P., and Piomelli, D. (1997). A second endogenous cannabinoid that modulates long-term potentiation. Nature *388*, 773–778.

Sugiura, T., Kondo, S., Sukagawa, A., Nakane, S., Shinoda, A., Itoh, K., Yamashita, A., and Waku, K. (1995). 2-Arachidonoylglycerol: a possible endogenous cannabinoid receptor ligand in brain. Biochem. Biophys. Res. Commun. *215*, 89–97.

Ueda, N., Yamanaka, K., and Yamamoto, S. (2001). Purification and characterization of an acid amidase selective for N-palmitoylethanolamine, a putative endogenous anti-inflammatory substance. J. Biol. Chem. *276*, 35552–35557.

Zvonok, N., Pandarinathan, L., Williams, J., Johnston, M., Karageorgos, I., Janero, D.R., Krishnan, S.C., and Makriyannis, A. (2008). Covalent inhibitors of human monoacylglycerol lipase: ligand-assisted characterization of the catalytic site by mass spectrometry and mutational analysis. Chem. Biol. *15*, 854–862.